Available online at www.sciencedirect.com

ScienceDirect

Physics Procedia 69 (2015) 130 – 137

Physics Procedia

10 World Conference on Neutron Radiography 5-10 October 2014

Development and Test of a Neutron Imaging Setup at the PGAA Instrument at FRM II

S. Söllradl*[a,b], M. J. Mühlbauer[a,c], P. Kudejova[a], A. Türler[b]

[a]*Maier-Leibnitz Zentrum (FRM II), Technische Universität München, Lichtenbergstraße 1, D-85748 Garching, Germany*
[b]*Laboratory of Radiochemistry and Environmental Chemistry, Paul Scherrer Institut, CH-5232 Villigen PSI, Switzerland*
[c] *Institute for Applied Materials (IAM), Karlsruhe Institute of Technology (KIT), , Hermann-von-Helmholtz-Platz 1, D-76344 Eggenstein-Leopoldshafen, Germany*

Abstract

We report on the developments of a neutron tomography setup at the instrument for prompt gamma-ray activation analysis (PGAA) at the Maier-Leibnitz Zentrum (MLZ). The recent developments are driven by the idea of combining the spatial information obtained with neutron tomography with the elemental information determined with PGAA, i.e. to further combine both techniques to an investigative technique called prompt gamma activation imaging (PGAI). At the PGAA instrument, a cold neutron flux of up to 6 x 10^{10} cm^{-2} s^{-1} (thermal equivalent) is available in the focus of an elliptically tapered neutron guide. In the reported experiments, the divergence of the neutron beam was investigated, the resolution of the installed detector system tested, and a proof-of-principle tomography experiment performed.
In our study a formerly used camera box was upgraded with a better camera and an optical resolution of 8 line pairs/mm was achieved. The divergence of the neutron beam was measured by a systematic scan along the beam axis. Based on the acquired data, a neutron imaging setup with a L/D ratio of 200 was installed. The resolution of the setup was tested in combination with a gadolinium test target and different scintillator screens. The test target was irradiated at two positions to determine the maximum resolution and the resolution at the actual sample position. The performance of the installed tomography setup was demonstrated by a tomography experiment of an electric amplifier tube.

Selection and peer-review under responsibility of Paul Scherrer Institut

Keywords: Neutron imaging, Instrumentation, PGAA,PGAI, Divergence measurement

* Corresponding author. Tel.: +49-89-289-14768; fax: +49-89-289-14911.
E-mail address: Stefan.soellradl@frm2.tum.de

Selection and peer-review under responsibility of Paul Scherrer Institut
doi:10.1016/j.phpro.2015.07.019

1. Introduction

The palette of techniques available in the field of neutron imaging has significantly increased in recent years. Especially with the development of digital image processing, the availability and development of strong neutron sources(Lehmann, 2014) in combination with ongoing research gave rise to a broad number of techniques like stroboscopic imaging(Schillinger et al., 2006; Tremsin et al., 2010) energy selective imaging(Peetermans et al., 2014), and imaging techniques with polarized neutrons(Kardjilov et al., 2014; Lehmann, 2014; Schulz et al., 2011; Treimer, 2014). Another promising technique investigated recently, is prompt gamma-ray activation imaging(PGAI)(Belgya et al., 2008), a combination of the analytical technique of prompt gamma-ray activation analysis (PGAA)(Molnár, G.L. (ed.), 2004) and neutron imaging (NI) for an element sensitive visualization of the sample. The general feasibility of PGAI was investigated already during the ANCIENT CHARM project(Schulze et al., 2013). However, until now an automatic scanning and data-merging of the acquired data is not available and requires strong user interaction, especially for image preparation and data merging. After the ANCIENT CHARM project, the development of such a system was continued at the research reactor in Budapest(Belgya et al., 2008) as well as at MLZ(Canella et al., 2009) with the goal of developing a permanent setup for automated investigations of small and inhomogeneous samples.

The reported study was performed at the PGAA instrument at MLZ(Canella et al., 2011), which is located at the end of a curved neutron guide. Its last few meters are elliptically tapered in horizontal and vertical direction. At the present PGAA instrument, only a small space of approximately 850 mm is available for the installation of a neutron imaging setup and is thus, the limiting factor for the L/D ratio and the illuminated image area of the setup.

At the PGAA instrument, two options are available for the modification of the incident beam at the end of the main neutron guide(Revay et al., 2015). One is a flight tube, while the other is an elliptical extension which can be introduced into the beam. Especially the application of the elliptical extension offers a great potential for a future imaging setup as the area around the focus can be accessed easily and due to the high flux and divergence a small pin-hole aperture can be mounted for an imaging setup.

In the frame of this study, we report about recent developments towards an imaging setup at the PGAA instrument with regard to the different possible beam options available. Until now just a few sections of the neutron beam were characterized(Kudejova 2008, Ebert 2008) and a systematic study is still pending. For this investigation, we upgraded an available camera box(M. J. Mühlbauer et al., 2005), with a 16-bit CCD camera and mounted it on a linear stage. The linear stage was fixed on the PGAA instrument and scans along the neutron beam were performed. From the acquired image series, the intensity-width profiles of the neutron beam were determined and the divergence calculated with the prospect of installing a future imaging system. Based on the obtained data, a preliminary tomography setup was installed with an L/D ratio of 200 and a first tomography of an electric amplifier tube was performed.

2. Experimental

All experiments were performed at the PGAA instrument, located at the Maier-Leibnitz Zentrum (MLZ) in Garching. The facility is located at a distance of about 51 m from the reactor core at the end of a strongly curved (radius of 390 m) neutron guide pointing on the cold-neutron source(Kudejova et al., 2008). The last section of the guide (seen from the reactor towards the instrument) with a length of 6.9 m is kept straight and is elliptically tapered in both, the horizontal and vertical direction. At the end of this neutron guide, two irradiation options are available. Either a flight tube with a straight collimation of 1000 x 20 x 20 mm^3 or an elliptical extension, with a total length of 1090 mm can be introduced into the beam (illustrated in Fig. 1a). The components belonging to the neutron guide and indicated in Fig. 1a are usually surrounded by heavy shielding, visible on the right part of Fig. 1a. At the end of this shielding, a linear moving stage was installed as illustrated in Fig. 1b. The stage was constructed in a way, that the front face of the camera could touch the shielding material at the end of the neutron guide. This position is defined as the 0 mm reference position for all scanning experiments. During these scans, the stage was equipped with an upgraded DEL-Cam housing(J. Mühlbauer, 2005) and equipped with a 300 μm LiF/ZnS scintillator. On top of the DEL-Cam housing, an Andor® DWZ436 CCD camera with a chip size of

2048x2048 pixel^2 and 16-bit readout was mounted. The camera chip was maintained at a temperature of -40°C and one pixel corresponded to a distance of 41 µm on the scintillator screen. The whole camera box was moved along the beam axis during a single scan and images were acquired in regular intervals.

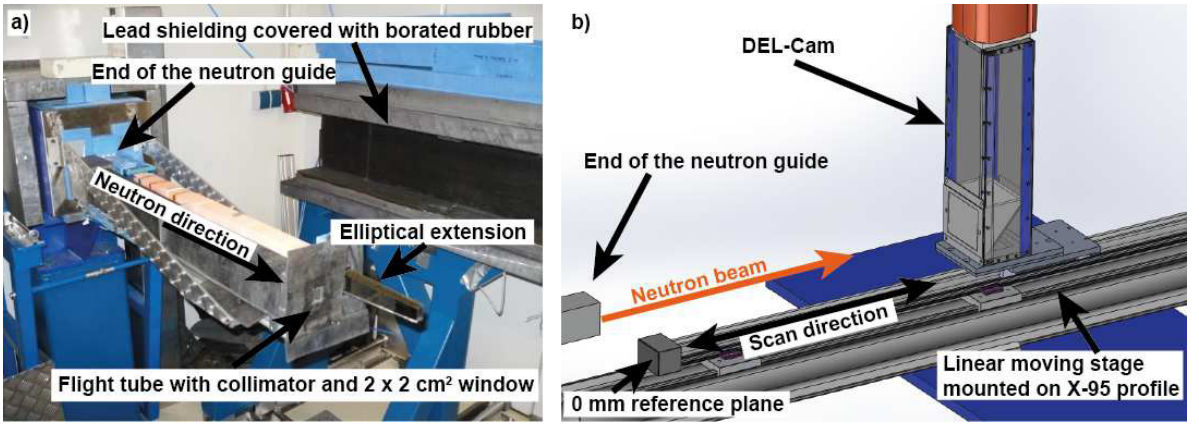

Fig. 1 (a) Image of the two possible beam options at the end of the neutron guide at the PGAA instrument; (b) Schematic image of the experimental setup as it was installed for the investigation of the neutron beam (except shielding materials).

Scanning of the beam profile using the collimator was performed without any additional attenuators. It started at a distance of 50 mm behind the shielding of the neutron guide. The camera box was moved in intervals of 20 mm per step and images were acquired with exposure times of 0.2 s. In contrast to that, an additional attenuator had to be used for the experiments with the elliptical extension for radiation protection reasons. The so called "Attenuator 1"(Canella et al., 2011), containing a profile of vertical slits, was placed in the beam, reducing the incident neutron beam to 17 % of its initial intensity. The performed scan with the elliptical extension started closely behind the focus of the guide at a distance of 50 mm from the lead shielding. It was performed in steps of 20 mm, covering a total distance of 400 mm. During the experiment images were acquired with an exposure time of 1.0 s. More details about the geometry of the used attenuators can be found in the appendix of (Söllradl, 2014). The intensity profiles were determined by averaging each row of pixels over a width of 120 pixels for the vertical profile and each column over a height of 120 pixels for the horizontal profiles, respectively (see Fig. 2). To determine applicable intensity for an imaging experiment, a brightness of 5% from the maximum intensity was assumed. This approach was benchmarked by determining the beam divergence using the neutron collimator with a defined geometry and applied for the elliptical extension as well.

Based on this geometric investigation of the neutron beam, a neutron tomography setup was developed. Therefore the translation unit was removed and a high-precision xyzω-positioning unit manufactured by the company XHuber was installed below the PGAA setup. The carriage of the instrument was moved backwards in the direction of the neutron beam to its outmost position. In the empty space between the carriage and the end of the neutron guide, a boron carbide aperture (4 mm pinhole diameter) was installed in the focus of the elliptical extension. The detector box was mounted at a distance of 800 mm from this aperture and the center of the sample rotation was fixed due to constructional reasons at a distance of 30 mm in front of the scintillator screen. The tomography experiment was performed with a 100 µm LiF/ZnS screen, mounted in the camera box described above. The exposure time during the tomography was set to 2.2 s per image and 375 images were recorded over a total of 360 degrees. The images were reconstructed using the software Octopus 8.6(Inside Matters, 2013) in cone-beam geometry and visualized with VG StudioMax 2.2(Volume Graphics GmbH, 2013).

3. Results and Discussion

Fig. 2 shows the false-color images of the acquired images of the neutron beam at the PGAA instrument, using the elliptical extension of the guide and neutron "Attenuator 1". The white rectangles indicate the areas, in which the intensity profiles were determined for the elliptical extension. Fig. 2a shows the intensity of the neutron beam at a distance of 110 mm from the reference plane indicated in Fig. 1. The determination of the intensity profiles was continued up to a distance of 450 mm from the reference plane which is shown in Fig. 2b. Due to the inhomogeneity of the beam profile, only the first part of the scan was taken into account for the determination of the neutron-beam divergence (Fig. 3).

A similar series of beam-intensity profiles was recorded, using the neutron collimator. The corresponding horizontal and vertical widths for both setups (collimator and elliptical extension) at an intensity of 5% of the maximum brightness are plotted as a function of the distance from the lead shielding in Fig. 3.

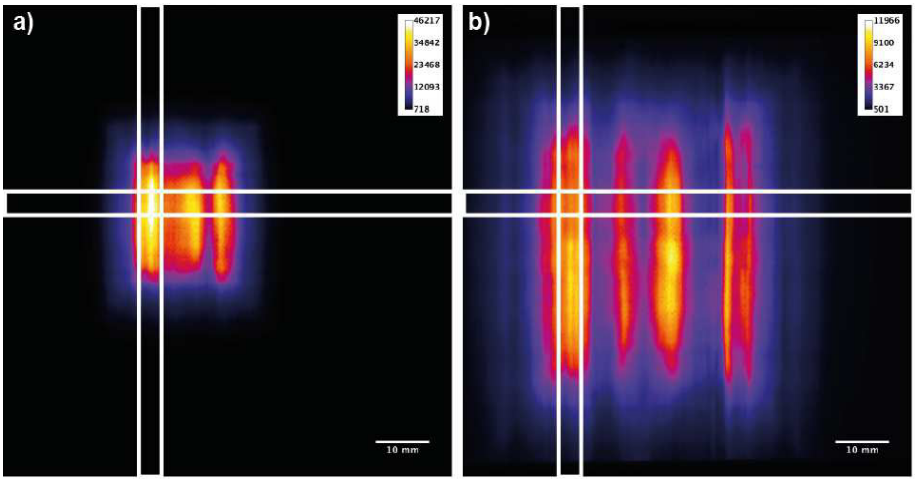

Fig. 2: False-color images of the neutron beam, using the elliptical extension at different distances from the end of the neutron guide. The white rectangles indicate the regions which were taken into account for the determination of the beam divergence. a) intensity of the beam at a distance of 110 mm from the reference plane at the lead shielding; b) intensity at a distance of 450 mm from the reference plane.

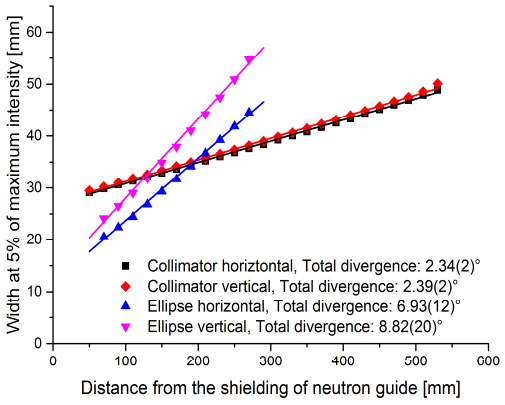

Fig. 3: Intensity profiles and determined beam divergence angles for the different setups available at the PGAA instrument

Each set of data was fit with a linear regression function. The divergence was then calculated according to

$$\alpha = \tan^{-1}(m) \tag{1}$$

where α is the opening angle of the neutron beam and m is the slope of the regression function. The expected opening angle for the neutron collimator, given with a length of 1000 mm and a diameter of 20 mm was calculated to be 2.3° (see schematic sketch in Fig. 4). Well in agreement are the experimentally determined values for the opening angle of 2.34(2)° in horizontal direction and 2.39(2)° in vertical direction (Fig. 3), also confirming the method to be suitable for the determination of the beam divergence of the elliptical extension.

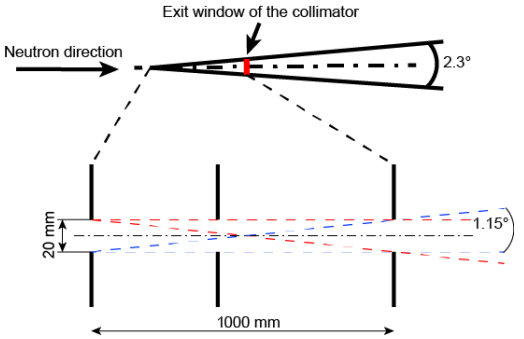

Fig. 4: Schematic drawing of the neutron collimator at the PGAA instrument and the expected angles for the beam divergence

In the case of the elliptical extension, the values of the horizontal and vertical divergence vary significantly. The smaller divergence of 6.93° in horizontal direction, compared to the 8.82° in vertical direction, can be attributed to the strong curvature of the neutron guide. At the moment simulations are in progress, which are expected to explain the observed intensity pattern as well as the different divergence angles. After the completion of those, the results will be reported elsewhere.

Based on the measured beam divergences for both options, in combination with the limited space available at the experimental area inside the bunker of the PGAA instrument, the elliptical extension was chosen as the preferred setup for neutron imaging. A divergence of 6.93° in horizontal and 8.82° in vertical direction will result in an illuminated area of approximately 97 mm and 124 mm, respectively. Those dimensions are limiting the maximum size of samples that can be investigated. The first investigation with the assembled imaging setup was an optimization between the necessary exposure time and the possible resolution without the application of a neutron attenuator. For this reason the images of a Siemens star on a gadolinium test target(Grünzweig et al., 2007) were investigated and compared (Fig. 5).Fig. 5a shows the complete structure of the Siemens star of the test device, acquired with a 10 µm Gadox scintillator. A magnified section of this image is shown for comparison in Fig. 5b. The thin scintillator screen required exposure times of 30 s but was used to minimize the effect of the scintillator thickness on the spatial resolution. The structures of the Siemens star were identified almost to the last quarter in the inner section close to the 100 µm marker of the star. It is in good agreement with the determined resolution of an earlier study(Söllradl, 2014), where a resolution of 8.0 line pairs/mm was measured using an optical test target. The lower images (Fig. 5c and d) show the structure of the Siemens star at a distance of 40 mm from the scintillator screen for different scintillator materials and thicknesses. It is intended to simulate the worst case for the projection of a detectable structure inside a small sample (assumed diameter of 20 mm) and mounted on the sample holder with a rotation axis at a distance of 30 mm from the scintillation screen. In the described case, the L/D ratio becomes the limiting parameter for the resolution and blurring can be approximated by

$$d = x \times (L/D)^{-1}, \tag{2}$$

where *d* is the diameter of the projection of a point in the sample on the scintillation screen, that is located at distance *x* from the front of the screen and projected with an instrument of a certain L/D ratio. In the case of the tested setup, a resolution of 200 µm was expected and could be confirmed by the experiment.

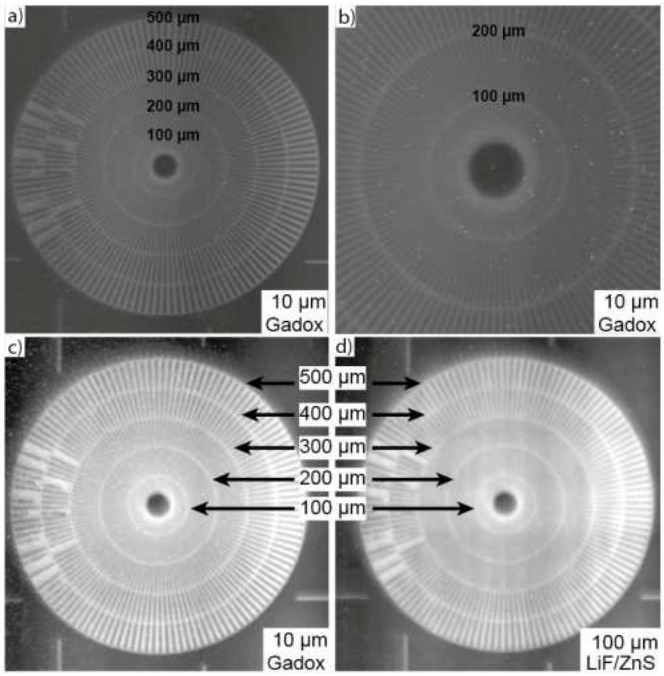

Fig. 5: Resolution measurement performed with the Siemens star structures. Image a) and b) shows the image of the test structure with contact to the used 10 µm Gadox screen; b) is a detailed view of the inner section of image a). The lower images c) and d) show the structure of the test target, positioned at a distance of 40 mm from the scintillator screen; c) on a 10 µm Gadox screen; (d) on a 100µm LiF/ZnS screen

Using the 10µm thick Gadox screen (Fig. 5c) structures until almost 200 µm could be detected, while a resolution of 250 µm was possible with the 100 µm thick LiF/ZnS screen (Fig. 5d).However, the exposure time of 2.2 s with the LiF/ZnS screen was significantly lower compared to an acquisition of images with similar brightness using the Gadox screen, requiring 30 s. Hence a lower resolution by 50 µm was accepted for the first tomography experiment and the setup was optimized for exposure time, which could be reduced by a factor of almost 14, also reducing the sample activation.

Fig. 6 shows the electric amplifier tube, which was used for the proof-of-principle measurement. Fig. 6a shows the real sample with a height of 5 cm and a diameter of 1.8 cm. The amplifier tube inherited various small structures which could be successfully visualized by the tomography. In the presented case, 817 projections were necessary to fulfill the sampling theorem completely. However, due to the limited time for testing the tomography setup and the relatively long readout of the camera data, 5 times longer than the acquisition, only 375 projections (plus one additional at 180.00°) were acquired. The materials composition of the tube allowed a sufficient transmission of the cold neutron beam for all angular orientations. Fig. 6b and 6c show the corresponding tomographs after the reconstruction of the amplifier tube. The overview of the sample is shown in Fig. 6b and a clipping box revealed its inner structures, which were not visible from the outside. The obvious grid structure surrounding the inner components as well as the different connectors and metal sheets were visualized clearly. By further clipping of the reconstructed data in the lower section of the sample (Fig. 6c) even the heating wires inside of the cathode were resolved.

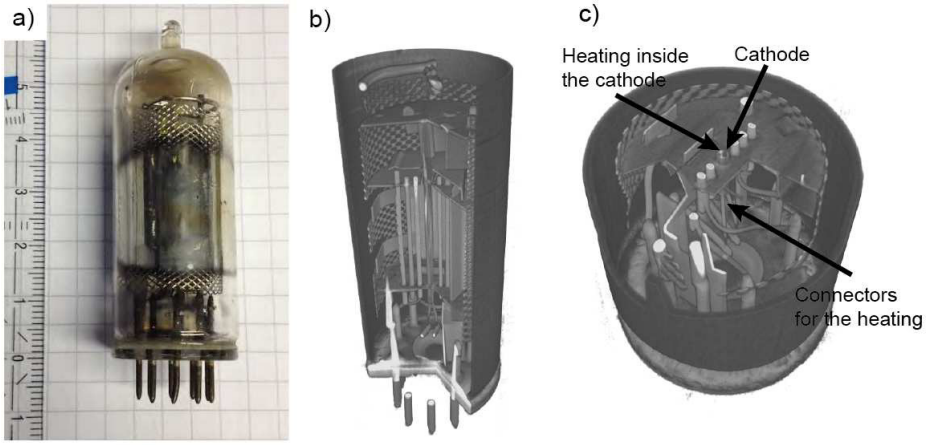

Fig. 6: a) Image of the investigated electric amplifier tube; b) Neutron tomography with a vertical cut-out; c) Magnified and clipped section of the connector section of the amplifier tube.

4. Conclusion

In the presented study a systematic investigation of the beam intensity profiles at the PGAA instrument at MLZ was performed and the beam divergences were determined from intensity profiles recorded along the neutron beam. A method was successfully tested to determine the divergence of the beam, based on a profile width of 5% of the maximum beam brightness. The developed method was benchmarked with a neutron collimator in place and confirmed the expected values of 2.3° divergence. It was found, that the divergence of the neutron beam differs in horizontal and vertical direction by using the elliptical extension and can be given with 6.92(12)° and 8.82(20)°, respectively. The obtained data showed, that in consideration of the limited space, the elliptical extension should be used for a neutron imaging setup at the PGAA instrument. A good compromise between the resolution and exposure time was found, by the application of a 100 µm LiF/ZnS scintillator screen. Based on these findings, a neutron imaging setup, utilizing the elliptical extension, was installed with a pinhole diameter of 4 mm and an L/D ratio of 200. Its performance was successfully proven by computed tomography of an electric amplifier tube.

Acknowledgements

The authors would like to express their gratitude to thank Michael Schulz, Burkhard Schillinger, Anders Kästner and N. Kardjilov for the many discussions about neutron imaging during the ITMNR-7 conference in Kingston, Canada. They would also like to thank Ümit Ünsal, Tudor Olariu and Eschly Kluge for the support during the first measurement campaign and for installing the scanning device.

References

Belgya, T., Kis, Z., Szentmiklósi, L., Kasztovszky, Z., Festa, G., Andreanelli, L., Pascale, M.P., Pietropaolo, A., Kudejova, P., Schulze, R., Materna, T., the Ancient Charm Collaboration, 2008. A new PGAI-NT setup at the NIPS facility of the Budapest Research Reactor. J. Radioanal. Chem. 278, 713-718.

Canella, L., Kudejova, P., Schulze, R., Tuerler, A., Jolie, J., 2011. Characterisation and optimisation of the new Prompt Gamma-ray Activation Analysis (PGAA) facility at FRM II. Nucl Instrum Meth A 636, 108-113.

Canella, L., Kudejova, P., Schulze, R., Türler, A., Jolie, J., 2009. PGAA, PGAI and NT with cold neutrons: Test measurement on a meteorite sample. Applied Radiation and Isotopes 67, 2070-2074.

Ebert, M, 2009. Untersuchung archäologischer Objekte mit Neutronen, Diploma Work, University of Cologne

Grünzweig, C., Frei, G., Lehmann, E., Kühne, G., David, C., Grünzweig, C., Kühne, G., 2007. Highly absorbing gadolinium test device to characterize the performance of neutron imaging detector systems. Rev. Sci. Instrum. 78, 053708.

Inside Matters, 2013. Octopus (Version 8.6) [Software]

Kardjilov, N., Hilger, A., Manke, I., Banhart, J., 2014. CONRAD-2: The neutron imaging instrument at HZB. Neutron News.

Kudejova, P., Meierhofer, G., Zeitelhack, K., Jolie, J., Schulze, R., Turler, A., Materna, T., 2008. The new PGAA and PGAI facility at the research reactor FRM II in Garching near Munich. J. Radioanal. Chem. 278, 691-695.

Lehmann, E., 2014. NEUWAVE-6: Progress and Perspectives in Neutron Imaging. Neutron News.

Molnár, G.L. (ed.), 2004. Handbook of Prompt Gamma Activation Analysis with Neutron Beams. Kluwer Academic Publishers.

Mühlbauer, J., 2005. Bau eines Entwicklungssystems für Radiographie und Tomographie mit Neutronen, Building μTOS. Technische Universität München.

Mühlbauer, M.J., Calzada, E., Schillinger, B., 2005. Development of a system for neutron radiography and tomography. Nucl Instrum Meth A 542, 324-328.

Peetermans, S., Tamaki, M., Hartmann, S., Kaestner, A., Morgano, M., Lehmann, E.H., 2014. A new transmission based monochromator for energy-selective neutron imaging at the ICON beamline. Nuclear Instruments and Methods in Physics Research Section A: Accelerators, Spectrometers, Detectors and Associated Equipment 757, 28-32.

Revay et al., 2015. publication in preparation.

Schillinger, B., Brunner, J., Calzada, E., 2006. A study of oil lubrication in a rotating engine using stroboscopic neutron imaging. Physica B 385-386, 921-923.

Schulz, M., Schmakat, P., Franz, C., Neubauer, A., 2011. Neutron depolarisation imaging: Stress measurements by magnetostriction effects in Ni foils. Physica B: Condensed.

Schulze, R., Szentmiklósi, L., Kudejova, P., Canella, L., Kis, Z., Belgya, T., Jolie, J., Ebert, M., Materna, T., Biró, K.T., Hajnal, Z., 2013. The ANCIENT CHARM project at FRM II: three-dimensional elemental mapping by prompt gamma activation imaging and neutron tomography. Journal of Analytical Atomic Spectrometry 28, 1508.

Söllradl, S., 2014. Developments in prompt gamma-ray neutron activation analysis and cold neutron tomography and their application in non-destructive testing. Universität Bern.

Treimer, W., 2014. Radiography and tomography with polarized neutrons. Journal of Magnetism and Magnetic Materials.

Tremsin, A.S., Muhlbauer, M.J., Schillinger, B., McPhate, J.B., Vallerga, J.V., Siegmund, O.H.W., Feller, W.B., 2010. High Resolution Stroboscopic Neutron Radiography at the FRM-II ANTARES Facility. IEEE Trans. Nucl. Sci. 57, 2955-2962.

Volume Graphics GmbH, 2013. VG Studio Max (Version 2.2) [Software].